PHYSICAL REVIEW B VOLUME 55, NUMBER 9 1 MARCH 1997-I

First-principles molecular-dynamics simulation of liquid rubidium under high pressures

Fuyuki Shimojo
Faculty of Integrated Arts and Sciences, Hiroshima University, Higashi-Hiroshima 739, Japan

Y. Zempo
Sumitomo Chemical, 6 Kitahara, Tsukuba 300-32, Japan

Kozo Hoshino and Mitsuo Watabe
Faculty of Integrated Arts and Sciences, Hiroshima University, Higashi-Hiroshima 739, Japan

(Received 1 July 1996; revised manuscript received 5 November 1996)

The effects of compression on the structural and electronic properties of liquid rubidium are studied along the melting curve by means of a first-principles molecular-dynamics simulation. It is shown that the calculated pair distribution functions $g(r)$ are in good agreement with the experimental results for a wide range of pressures; the liquid rubidium is compressed uniformly at 2.5 GPa, and there exist some deviations from the uniform compression at 6.1 GPa. This structural change to a denser state is related to an electronic s-d transition in the liquid state. It is found that, near the triple point, the electronic density of states consists mostly of the s component and, with increasing pressure, the s component decreases gradually over a wide range of energy, and the d component near the Fermi level increases. [S0163-1829(97)06509-0]

In recent papers,[1,2] we have reported on the results of the first-principles simulation of expanded liquid rubidium, and clarified the characteristic features with decreasing density along the liquid-vapor coexistence curve. The relation between the temperature dependence of the electron density distribution $\rho(r)$ and the disordered configuration of ions has been examined, and it has been shown that, at high temperatures, $\rho(r)$ tends to localize due to the large spatial fluctuation of atomic density, while, near the triple point, it spreads over all space.

On the other hand, we can study changes in the structural and electronic properties with increasing density, if we go up towards higher pressure states along the melting curve, and there have been some experimental attempts in this respect. Recently, Tsuji *et al.*[3] have measured the pressure dependence of the static structure factor $S(k)$ of liquid cesium by x-ray-diffraction experiments. They have found that two transitions occur in the liquid state. One is a transition from a bcc-like structure to an fcc-like structure at about 2 GPa, and the other is a transition to a denser structure at 3~4 GPa. They have discussed these transitions in relation to the pressure-induced phase transition in crystal cesium and the $6s$-$5d$ electronic transition. More recently, they have measured the $S(k)$ of liquid rubidium by x-ray diffraction at pressures up to 6.1 GPa along the melting curve.[4] It has been found, by investigating $S(k)$ and the pair distribution function $g(r)$, that the liquid rubidium is compressed uniformly up to about 2.5 GPa, i.e., $V/V_0=0.7$, where V_0 is the volume at an ambient pressure; however a deviation appears from a uniform compression at higher pressures. The first-peak position of $S(k)$ changes slightly less than the expectation, and the first coordination number increases.

In a solid state under pressure, the heavy alkali metals exhibit a bcc→fcc transition before they transform into more complex structures at higher pressures.[5–7] From theoretical studies,[8–12] it has been pointed out that the occupation of the d valence band plays an important role in these phase transitions. The basic microscopic mechanism of this electronic s-d transition in solid phases has been understood by band structure calculations.[8,12] So far, however, the electronic transtion in liquid phase under compresstion has not been clarified yet.

In the present paper, we investigate the structural and electronic properties of liquid rubidium under pressure by the first-principles molecular-dynamics (MD) simulation. The purposes of this paper are as follows: (i) to compare the structural results obtained by our simulation with recent experiments by Tsuji *et al.*,[4] and (ii) to examine how the electronic s-d transition occurs in the liquid state.

Our calculations are performed within the framework of the density functional theory utilizing the local density approximation.[13] Electronic wave functions are expanded in the plane-wave (PW) basis set. The energy functional is minimized for each ionic configuration using an iterative scheme based on the preconditioned conjugate-gradient method.[14–16] The fractional occupancy of each state is taken into account in applying the first-principles MD simulation to the liquid metals.[17] Since we need a large PW cutoff energy to expand the deep d pseudopotential in the case of a conventional norm-conserving pseudopotential,[18] we use the ultrasoft pseudopotential proposed by Vanderbilt[19] to reduce the computational cost. The core correction[20] is included in our simulation.

Using the Nosé-Hoover thermostat technique,[21] the equations of motion are solved via the velocity Verlet algorithm with time step $\Delta t=4.8\times10^{-15}$ s. The supercell contains 54 rubidium atoms with periodic boundary conditions. The simulations are carried out at three different densities and

0163-1829/97/55(9)/5708(4)/$10.00

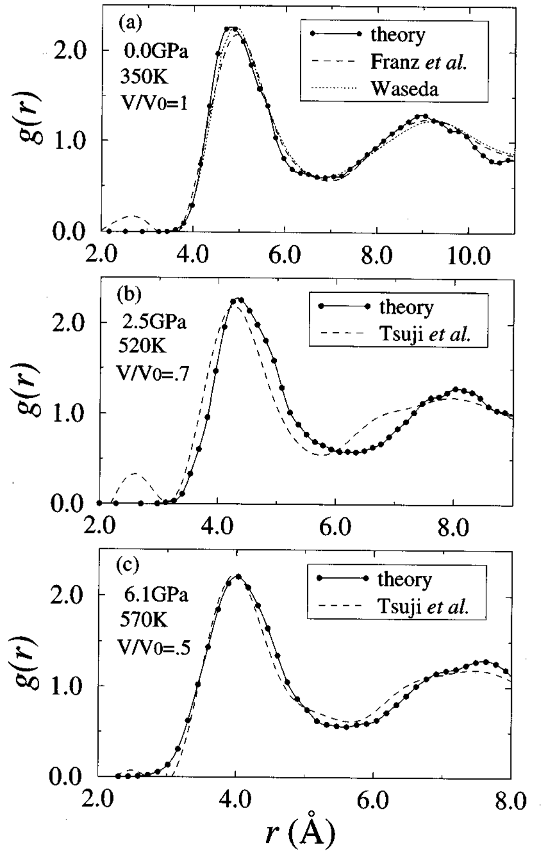

FIG. 1. The pair distribution functions $g(r)$ calculated at (a) (0 GPa, 350 K), (b) (2.5 GPa, 520 K), and (c) (6.1 GPa, 570 K), compared with the experimental results. The solid line shows the $g(r)$ obtained by these calculations. The dashed and dotted lines in (a) show the experimental results of Franz *et al.* (Ref. 22) and Waseda (Ref. 23), respectively. The dashed lines in (b) and (c) show the experimental results of Tsuji *et al.* (Ref. 4).

temperatures along the melting curve: (1.459 g/cm^3, 350 K) near the triple point, (2.055 g/cm^3, 520 K), and (2.850 g/cm^3, 570 K), which correspond to the pressures, 0, 2.5, and 6.1 GPa, respectively. Only the Bloch functions at the Γ point are used, and the wave functions and electron density are expanded in the plane waves with an energy cutoff of 5.5 and 50 Ry, respectively. The system is equilibrated during the first 2 ps in every simulation. The quantities of interest are obtained by averaging those over about 3 ps after this initial equilibration. During the simulations, the conserved quantities in the Nosé-Hoover dynamics are kept constant with fluctuations being less than 10^{-2} mRy/atom.

The pair distribution functions $g(r)$ calculated at 0, 2.5, and 6.1 GPa are shown, respectively, in Figs. 1(a), 1(b), and 1(c), and compared with the corresponding experimental results.[4,22,23] The calculations of $g(r)$ are extended up to distances equal to a half-diagonal of the supercells.[24] From Fig. 1(a), we see that the calculated result near the triple point is in good agreement with the experimental results. At higher pressures, the calculated results are also in agreement with the experimental results, though some deviations from the experimental results are recognized, especially for 2.5 GPa. The experimental $g(r)$ are obtained by a Fourier transformation of the static structure factors $S(k)$ which are directly measured by x-ray diffraction. Since the data of $S(k)$ in the small k region, $k < 1$ Å^{-1}, are not obtained by Tsuji *et al.*, the $g(r)$ derived from the experimental $S(k)$ has some ambiguities. We should notice that it is very difficult to determine accurately the density of liquid metals under high pressures. Considering these facts, we have succeeded in reproducing the structure of liquid rubidium for a wide range of pressures.

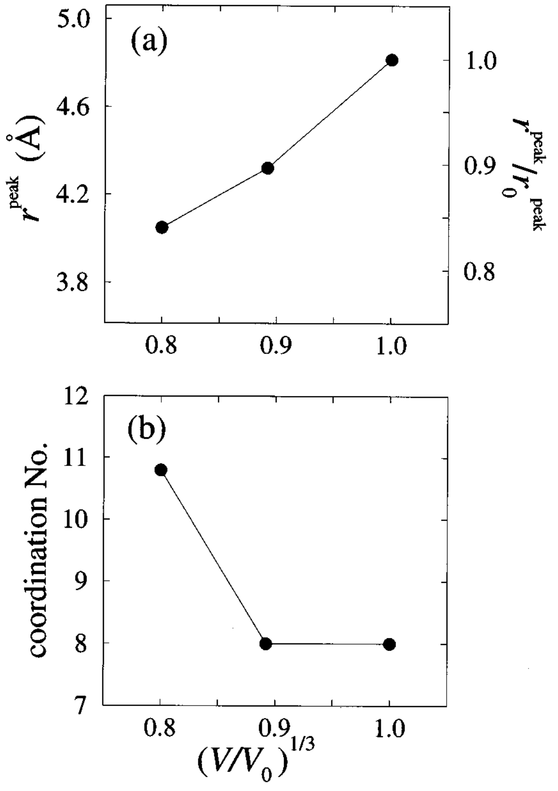

FIG. 2. (a) Position of the first peak $r^{\rm peak}$ ($r^{\rm peak}/r_0^{\rm peak}$) of the pair distribution function $g(r)$, and (b) the coordination number as a function of $(V/V_0)^{1/3}$, where $r_0^{\rm peak}$ and V_0 are the position of the first peak and the volume at an ambient pressure, respectively.

It is found that the position of the first peak shifts towards a smaller r under increasing pressure, and that the height of the first peak is almost unchanged though it decreases slightly at 6.1 GPa. These features are qualitatively different from the density dependence of the $g(r)$ along the liquid-vapor coexistence curve; when the density decreases from the triple point up to the critical point, the position of the first peak does not change, and its height decreases, causing the decrease of the coordination number. To examine the structural change in more detail, the position of the first peak $r^{\rm peak}$ of the $g(r)$ and the coordination number are plotted in Figs. 2(a) and 2(b), respectively, as functions of $(V/V_0)^{1/3}$. We define the coordination number as $2\rho\int_0^{r^{\rm peak}} 4\pi r^2 g(r)dr$. From Fig. 2(a), we see that the position of the first peak at 6.1 GPa deviates from the uniform compression, while there is no deviation at 2.5 GPa. It is found from Fig. 2(b) that the coordination number increases to about 11 at 6.1 GPa, while it is almost 8 at 0 and 2.5 GPa. Therefore, it is concluded that the liquid rubidium is compressed uniformly at 2.5 GPa, and

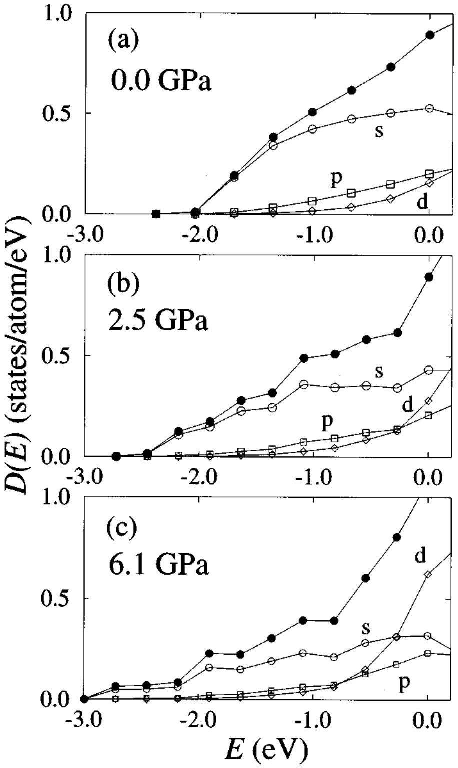

FIG. 3. Electronic density of states $D(E)$ and its l component $D_l(E)$ with $l=0$ (circle), 1 (triangle), and 2 (diamond) at (a) 0 , (b) 2.5, and (c) 6.1 GPa.

there exist some deviations from a uniform compression at 6.1 GPa, which means a structural change to a denser structure. These features are in good agreement with those suggested by Tsuji *et al.*[4]

Since an interest exists in clarifying the relation between the changes in the atomic configuration and the electronic states, we investigate the effects of compression on the electronic density of states (DOS).

The projected DOS $D_l(E)$ with l being the angular momentum is calculated from the one-electron energy with weighting factor, which is obtained by integrating wave functions projected by the spherical harmonics inside the sphere of radius R. The center of the sphere is the position of each atom. It should be noted that the radius R is arbitrarily chosen, and so the sum of $D_l(E)$ with respect to l is not equal to the total DOS $D(E)$. We choose almost the half distance of the closest approach as the value of R, i.e., $R=1.85$, 1.65, and 1.48 Å for 0, 2.5, and 6.1 GPa, respectively. When $D_l(E)$ were calculated with different values of R, we could obtain qualitatively similar results unless unphysically small values are chosen.

The Γ-point sampling in the first-principles MD simulation would not be satisfactory to describe details of the electronic structure such as the DOS, and it is important to recognize that adequate k-point sampling is essential. We therefore use the conventional ten k points with the appropriate weights in a cubic first Brillouin zone. The average is taken over five atomic configurations as well as ten k points.

In Fig. 3, $D(E)$ and $D_l(E)$ with $l=0,1$, and 2 are shown, where $D_l(E)$ are normalized so that the sum of $D_l(E)$ with respect to l gives $D(E)$. The origin of energy is taken to be the Fermi level. It is seen from Fig. 3(a) that, near the triple point, the total DOS $D(E)$ consists mostly of the s component, which has almost a $\sqrt{E}$ dependence, and that the p and d components are small. With increasing pressure and density, the s component decreases gradually over a wide range of energy, and the d component near the Fermi level increases, while the behavior of the p component is almost unchanged. At 6.1 GPa, the main contribution to $D(E)$ around the Fermi level is due to the d component as shown in Fig. 3(c). Thus, it is shown that the electronic s-d transition occurs gradually in the liquid rubidium, and that the structural change to a denser state at about 6.1 GPa is related to this electronic transition.

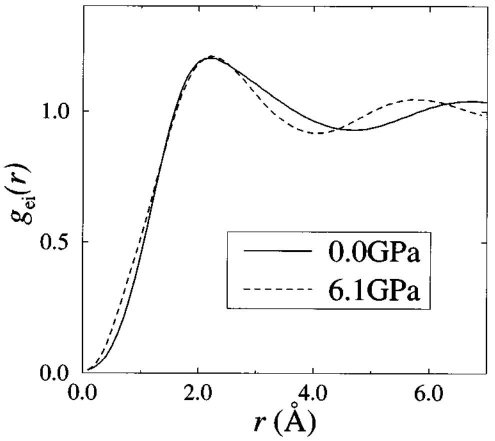

FIG. 4. Electron-ion correlation functions $g_{\mathrm{ei}}(r)$ at 0 (solid line) and 6.1 (dashed line) GPa.

In the previous paper,[1] the electron-ion pair correlation function $g_{\mathrm{ei}}(r)$ of the expanded liquid rubidium has been investigated in detail. To investigate the effects of compression on $g_{\mathrm{ei}}(r)$, we calculate $g_{\mathrm{ei}}(r)$, whose definition is given in Ref. 1, at 0 and 6.1 GPa, and the calculated $g_{\mathrm{ei}}(r)$ are shown in Fig. 4. As for the pressure dependence of $g_{\mathrm{ei}}(r)$, we can see the following characteristic features: (i) The position of the first peak of $g_{\mathrm{ei}}(r)$ does not change with increasing pressure, while the first minimum and the second maximum shift towards a smaller r, resulting from the fact that the position of the first peak of $g(r)$ shifts in the same way when the pressure is increased. (ii) With increasing pressure, the heights of the first and second peaks of the $g_{\mathrm{ei}}(r)$ do not change so much, which suggests that the correlation between the electronic and the ionic densities does not vary with the pressure. This feature is qualitatively different from that obtained when the liquid rubidium is expanded along the liquid-vapor coexistence curve.[1]

In summary, the effects of compression on the structural and electronic properties of liquid rubidium are studied by means of a first-principles molecular-dynamics simulation, in which the Kohn-Sham energy functional is minimized for each ionic configuration using the iterative scheme based on the preconditioned conjugate-gradient method. It is shown, by investigating the electronic density of states in detail, that the structural change to a denser state at 6.1 GPa is related to an electronic s-d transition in the liquid state. The pressure dependence of the electron-ion pair correlation function $g_{\mathrm{ei}}(r)$ is also discussed.

This work was supported by a Grant-in-Aid for Scientific Research on Priority Areas (No. 07236102) and for Encouragement of Young Scientists (No. 08740286) from The Ministry of Education, Science and Culture. The authors thank the Supercomputer Center, Institute for Solid State Physics, University of Tokyo for the facilities and the use of the FACOM VPP500. Numerical calculations were also carried out on the NEC SX-3/44R supercomputer at the Computer Center of Tohoku University.

---

[1] F. Shimojo, Y. Zempo, K. Hoshino, and M. Watabe, Phys. Rev. B **52**, 9320 (1995).

[2] F. Shimojo, Y. Zempo, K. Hoshino, and M. Watabe, J. Non-Cryst. Solids (to be published).

[3] K. Tsuji, K. Yaoita, M. Imai, T. Mitamura, T. Kikegawa, O. Shimomura, and H. Endo, J. Non-Cryst. Solids **117/118**, 72 (1990).

[4] K. Tsuji, Y. Katayama, Y. Morimoto, and O. Shimomura, J. Non-Cryst. Solids (to be published).

[5] H. T. Hall, L. Merril, and J. D. Barnett, Science **146**, 1297 (1964).

[6] K. Takemura and K. Syassen, Phys. Rev. B **28**, 1193 (1983).

[7] M. Winzenick, V. Vijayakumar, and W. B. Holzapfel, Phys. Rev. B **50**, 12 381 (1994).

[8] R. Sternheimer, Phys. Rev. **78**, 235 (1950).

[9] J. Yamashita and S. Asano, J. Phys. Soc. Jpn. **29**, 264 (1970).

[10] A. K. McMahan, Phys. Rev. B **29**, 5982 (1984).

[11] H. L. Skriver, Phys. Rev. B **31**, 1909 (1985).

[12] A. K. McMahan, Physica B **139&140**, 31 (1986).

[13] D. M. Ceperley and B. J. Alder, Phys. Rev. Lett. **45**, 566 (1980); J. P. Perdew and A. Zunger, Phys. Rev. B **23**, 5048 (1981).

[14] M. P. Teter, M. C. Payne, and D. C. Allan, Phys. Rev. B **40**, 12 255 (1989).

[15] T. A. Arias, M. C. Payne, and J. D. Joannopoulos, Phys. Rev. B **45**, 1538 (1992).

[16] G. Kresse and J. Hafner, Phys. Rev. B **49**, 14 251 (1994).

[17] M. J. Gillan, J. Phys. Matter **1**, 689 (1989).

[18] D. R. Hamann, M. Schlüter, and C. Chiang, Phys. Rev. Lett. **43**, 1494 (1979).

[19] D. Vanderbilt, Phys. Rev. B **41**, 7892 (1990).

[20] S. G. Louie, S. Froyen, and M. L. Cohen, Phys. Rev. B **26**, 1738 (1982).

[21] S. Nosé, Mol. Phys. **52**, 255 (1984); W. G. Hoover, Phys. Rev. A **31**, 1695 (1985).

[22] G. Franz, W. Freyland, W. Gläser, F. Hensel, and E. Schneider, J. Phys. (Paris) Colloq. **41**, C8-194 (1980).

[23] Y. Waseda, *The Structure of Non-crystalline Materials* (McGraw-Hill, New York, 1980).

[24] D. N. Theodorou and U. W. Suter, J. Chem. Phys. **82**, 955 (1985).